

Study of reduced graphene oxide-based nanofluids properties for heat transfer applications

D. Vasudevan ^a, D. Senthil Kumar ^b, M. Venkatesan ^{c*}, A. Kumaravel ^a,
P. Dineshkumar ^d, A. Sankar ^e

^a Department of Mechanical Engineering, K.S. Rangasamy College of Technology, Tiruchengode – 637 215, Tamil Nadu, India.

^b Department of Mechanical Engineering, Sona College of Technology, Salem – 636 005, Tamil Nadu, India.

^c Department of Mechanical Engineering, Excel Engineering College, Komarapalayam, Nammakal – 637 303, Tamil Nadu, India.

^d Department of Agricultural Engineering, Kongunadu College of Engineering and Technology, Thottiam, Trichy – 621 215, Tamil Nadu, India.

^e Department of Agricultural Engineering, Dhirajlal Gandhi College of Technology, Kamalapuram, Salem – 636309, Tamil Nadu, India

Nanofluid, with its thermophysical properties, plays a crucial role in the heat transfer applications. Numerous research investigations made use of nanomaterials that were purchased from the manufacturer, that may lead to high costs. Hence, in this research, reduced graphene oxide (rGO) has been synthesized (method) from low-cost graphite to improve the heat transfer rate (HTR) of the nanofluid. Obtained rGO nanomaterial is further processed into rGO1 and rGO2 by thermal and irradiation methods respectively. Different characterization techniques are utilized to evaluate the prepared materials' characteristics. The rGO nanofluids are prepared with 0.0005, 0.001, 0.003, 0.005, and 0.007 wt. % concentrations of rGO1 and rGO2 nanomaterials using two-step methods. The prepared nanofluids exhibit high stability with the presence of oxygenated groups resting on end of rGO flakes. Brownian motion of rGO in the base fluid is responsible for a rise in surface tension and thermal conductivity. The viscosity of the nanofluids improves with concentration and Newtonian behavior.

(Received February 23, 2025; Accepted June 12, 2025)

Keywords: Reduced graphene oxide (rGO), Thermal conductivity, Surface tension, Viscosity

1. Introduction

Heat transfer enhancement in heat transfer (HT) systems perform a critical role in the industrial applications; nevertheless, the fluids for example ethylene glycol, oil, water, etc called conventional fluids [1]. In terms of HTR, the transport characteristics of traditional fluids have not demonstrated satisfactory performance. Improving base fluid's thermal conductivity is an effective method of raising HTR. By dispersing macro along with micro-sized particles in base fluids, numerous investigators have attempted to enhance the thermal conductivity. However, by adding micro and macro-sized particles some issues including clogging, pressure drop increase, stability issues, and agglomeration are found. Choi and Eastman have found new fluids namely "nanofluids" which have shown excellent stability and enriched in thermal conductivity than base fluids [2, 3]. The nanofluids are made with additives, that include carbon-based and metallic compounds, to raise their thermal conductivity. Improvement of the thermal conductivity is higher in carbon-based materials i.e. graphite, carbon nanotubes (CNTs), graphene, etc than in metallic relevant materials [17-18]. As per the earlier reports, carbon-based materials have proven to significantly enhance heat transfer more than metallic-based materials [3-4]. However, the thermal performance of nanofluids

* Corresponding author: venkatesanm1972@gmail.com
<https://doi.org/10.15251/DJNB.2025.202.633>

with graphene is still not yet investigated. Therefore, the graphene-relevant materials with thermal applications are a big challenge, presence of good transport properties. The thermal and electrical conductivity shows excellent due to its layers such as the single and multi-layer planer structure of graphene [5-6]. Graphene is considered an effective solid additive for HT applications because of its high thermal conductivity. Investigation has shown that graphene-based fluids achieve significant improvements in thermal conductivity in comparison with other additives like CNTs, carbon fibers, and graphite. The extremely low stability of graphene in water has significant impact on thermal applications. In general, the graphene-relevant nanofluids are poor in stability due to their hydrophobic nature; less solubility in water. However, the higher stability material namely rGO has excellent stability in base fluids because of presence of hydrogen bonding and highly active layers in surfaces [7].

Likewise, the thermal conductivity of the rGO is more efficient than metallic and carbon-based materials. Hence, in heat transfer applications, rGO exhibits a significant role when compared with metallic and relevant materials. The preparation of nanofluid can be accomplished through two distinct techniques: the one-step method as well as the two-step method. However, majority of researchers prefer two-step method for its easy processing and economic feasibility [8-9].

In the current experimental work synthesis of rGO by using highly pure graphite powder which is commercially available in the market. However, the reduced graphene oxide (rGO1) is synthesized

by a surfactant-free thermal method [12]. In addition, rGO1 is modified to rGO2 with enhanced thermal physical properties using microwave irradiation followed by an ultra-sonication process [9-10]. To confirm the natural properties of rGO, various characterization studies such as XRD, UV, FTIR, AFM, Raman spectra, and Zeta potential are conducted. It is then; that heat transfer applications of rGO1 and rGO2 are elaborately executed. The thermophysical and stability are analyzed with different concentrations of rGO1 and rGO2, such as 0.0005, 0.001, 0.003, 0.005, 0.007 wt. % respectively.

2. Experimental methods

Surfactant-free rGO and highly stable modified rGO were synthesized using chemical exfoliation followed by thermal reduction processes [12]. The synthesized rGO was further modified to enhance its thermophysical properties, and the detailed step-by-step procedure has been thoroughly described.

2.1. Chemical exfoliation method

Graphite flakes were oxidized using a chemical exfoliation approach. Initially, 3.5g of graphite flakes had been combined with a "9:1 mixture of the concentrated H_2SO_4 and H_3PO_4 (360:40 ml) along with 18.5 g of potassium permanganate (KMnO_4). At 35-40°C temperature, the mixture was stirred continuously" for 4-5hours to initiate a slightly exothermic reaction. Subsequently, for 12hours, reaction mixture was heated to 50°C temperature while being stirred. Afterwards, it was kept to cool down to the room temperature, taking approximately 45 minutes. Once cooled, 400ml of ice-cold distilled water along with 5ml of hydrogen peroxide (H_2O_2) were added for the reaction completion. The dark pink product changed to a mustard color. Finally, mixture was washed with 1 M HCl, then double-distilled water repeatedly until pH of the supernatant liquid attained neutral (~7). [15].

2.2. Graphene oxide (GO) exfoliation process

GO was exfoliated through a sonication process under ambient conditions for 30 minutes using strong ultrasonic wave irradiation (~40 Hz). This process produced a homogeneous brown dispersion, that was then employed for reduction. Resulting solution was dried in a vacuum oven at room temperature for 24hours to yield a fine powder. [15-17].

2.3. Thermally reduced graphene oxide

For four hours, the exfoliated GO powder was heated to 500°C at a rate of 2°C per minute in a muffle furnace. It was then kept to cool down within the furnace until temperature dropped to 40±5°C. All aforementioned steps were carried out under normal room atmosphere. This process resulted in the complete conversion of GO into rGO. Prepared nanomaterial is referred to as rGO1, representing thermally reduced GO [15].

2.4. Modification of rGO

To get enhancement in dispersion and stability of the prepared rGO, rGO1 was subject to continuous microwave irradiation for 3 hours and followed by a sonication process for 3 hours. After the process was completed, finally obtained powder was named rGO2 (denoted for irradiation process influenced rGO) [14].

2.5. Characterization of rGO

The dispersion stability of the synthesized rGO1 and rGO2 in deionized water was evaluated using “UV–visible spectroscopy (Cary 8454; Agilent, Singapore) along with a Zeta Potential Analyzer (Zetasizer Nano ZS, Malvern). Utilizing an X-ray diffractometer (X’Pert PRO; PANalytical, Netherlands) with CuK α radiation ($\lambda=1.5406 \text{ \AA}$ ”), the samples’ phase and crystalline structure were determined. At room temperature (298K), measurements were made throughout a 2 θ range of 20 to 80°. A particle size analyzer (Nanophox; Sympatec, Germany) as per DLS (dynamic light scattering) was employed to examine the PSD (particle size distribution) of nanopowders. “Fourier transform infrared spectroscopy (FTIR; Spectrum 100; PerkinElmer, USA) had been employed to identify functional groups in the nanopowders, with spectra recorded over a range of 4000–400 cm^{-1} . HRTEM (High-resolution transmission electron microscopy) images had been acquired utilizing a Gatan Quantum ER 965 imaging filter” coupled with a JEOL instrument (Japan). Atomic force microscopy was utilized to further analyze the materials' surface morphology (AFM; Innova, USA, version 7), providing detailed information about surface properties. Lastly, the Raman spectra of rGO1 and rGO2 were recorded using a LabRAM HR-800 spectrometer (HORIBA, “France).

3. Results and discussion

3.1. Characterization of rGO 1 and rGO 2

The XRD (X-ray diffraction) patterns of rGO1 and rGO2 samples are presented in the Fig. 1”, revealing the crystalline structure of the prepared rGO. A sharp peak at $2\theta=26.5^\circ$ as well as minor peaks at $2\theta=44^\circ$, 65° , 78° correspond to (002), (100), and (001) planes, indicating graphitic structure of rGO1. In contrast, rGO2 sample exhibits slightly increased peak intensity with sharper features and an absence of the minor peaks at $2\theta = 44^\circ$ and 65° . The combination of microwave irradiation and sonication techniques employed resulted in a highly pure graphitic structure. [7-9,17].

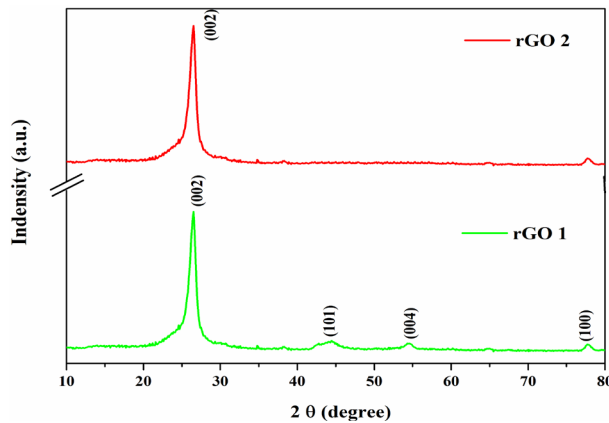


Fig. 1. a) XRD diffraction pattern of rGO 1 and rGO 2.

The experiential outcome suggests an improvement in the regularity of the graphitic structure in rGO, leading to better layer alignment in rGO2 compared to rGO1[7]. During the thermal reduction of GO, it had been reduced to rGO, and ordered crystal structure of rGO had been restored. According to the data, it is highly appropriate for heat transfer applications, as evidenced by the (002) diffraction peak reappearing at 26.5° and (001) diffraction peak disappearing.

Zeta potential, also known as electrophoretic potential, is an efficient method for assessing colloidal stability as well as agglomeration of solutions prepared using rGO1 and rGO2 [9]. Figure 2 illustrates the absolute zeta potential values of the highly stable colloidal solutions of rGO1 and rGO2 at room temperature (30°C). Typically, colloidal solutions with zeta potential values exceeding ± 30 mV are considered stable, as this prevents sedimentation and aggregation by ensuring ideal dispersion. The prepared colloids exhibit zeta potential values above the critical threshold of 30 mV, confirming their excellent stability and dispersion for heat transfer. As illustrated in Figure 2, absolute zeta potential values of rGO1 and rGO2 reach a maximum of -39 mV and -44 mV, respectively, at 30°C .

This specifies that prepared rGO exhibits enhanced dispersibility and prolonged stability in deionized water, a highly desirable property for producing stable nanofluids. This improved stability is likely attributed to the preparation methods used for rGO1 and the key influencing factors for rGO2, particularly the combination of microwave irradiation, followed by sonication, and the supernatant's compatibility with water. These methods enhance the stability of colloidal suspensions. Overall, results suggest that modifications in the preparation methods significantly impact particle aggregation and sedimentation in colloidal systems[6].

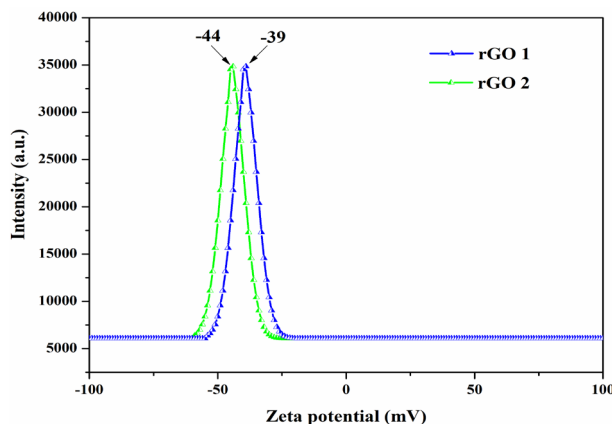


Fig. 2. Dispersion stability (Zeta potential) of rGO1 and rGO2.

Figure 3 presents the Raman spectra of rGO1 and rGO2. Raman spectroscopy is a highly effective technique for identifying structural defects in the carbon-based materials. D band, commonly associated with defect sites, provides insight into structural imperfections within the rGO framework. Specifically, D band observed at 1350cm^{-1} is characteristic of monolayer graphene. Structural defects in rGO nanoparticles (NPs) can influence their heat transfer properties, making Raman spectroscopy an essential method for analyzing these imperfections.

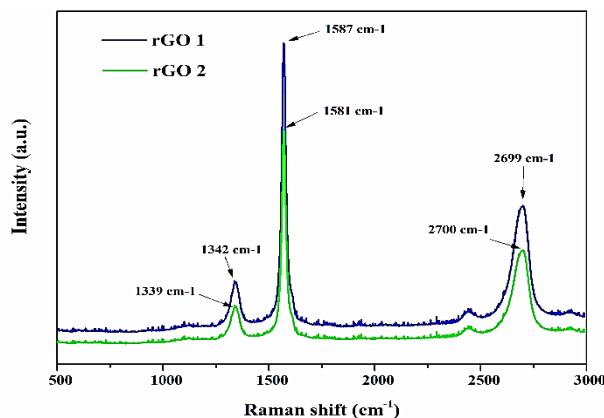


Fig. 3. Raman spectra of rGO1 and rGO2.

The presence of the D, G, 2D bands is distinctly detected at 1339 , 1581 , 2700cm^{-1} for rGO1 and at 1342 , 1587 , and 2699cm^{-1} for rGO2. These bands arise from in-plane stretching vibrations of sp^2 hybridized carbon atoms. The findings support the existence of graphene monolayers, that have been reported in the literature before. Notably, rGO2 exhibits sharper and more intense peaks compared to rGO1. The physical separation of graphene layers throughout the sonication and microwave processes is responsible for this improvement. [7,16].

The FTIR spectra of rGO1 and rGO2, exhibited in Figure 4, display similar absorption bands in range of $3410\text{--}3425\text{cm}^{-1}$, that are attributed to stretching vibrations of O–H groups. Distinct and sharp peaks at 2978 and 2855cm^{-1} for rGO1, and 2980 and 2849cm^{-1} for rGO2, correspond to C–H stretching vibrations. A weak peak observed at 1747cm^{-1} for rGO1 and 1746cm^{-1} for rGO2 indicates the presence of carboxylic and carboxylate group vibrations. Additionally, the peak at 1626cm^{-1} is associated with C=C stretching vibrations, while strong peaks at 1090cm^{-1} as well as 1082cm^{-1} are attributed to C=O stretching vibrations. [7].

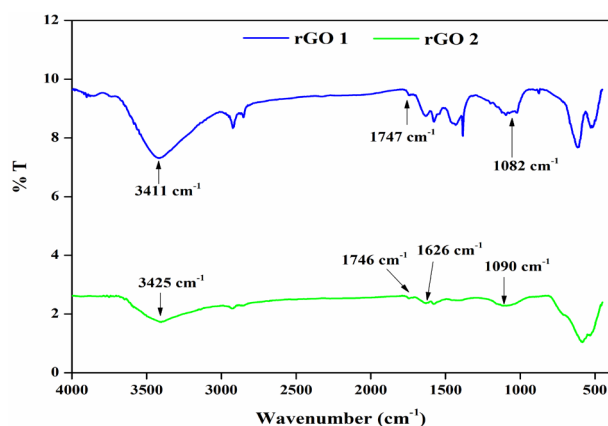


Fig. 4 Fourier transforms infrared spectra for the rGO1 and rGO2.

Particle size is a vital factor in enhancing HT. The average particle size of rGO1 and rGO2, measured using DLS, is presented in Figure 5. Based on the PSD acquired from the DLS analysis, hydrodynamic diameter of rGO1 and rGO2 ranges between 20 and 28 nm, with high concentration values (d_{50}) at 22.9nm and 27.1nm, correspondingly. Smaller average particle size of rGO2 compared to rGO1 is attributed to the thermal exfoliation process of graphene. Furthermore, the sonication process contributes to further reducing the particle size into the nanoscale range [14-16].

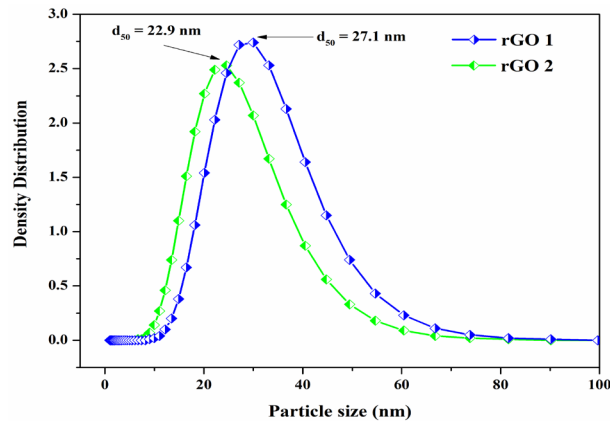


Fig. 5 Particle size distribution of the rGO 1 and rGO 2.

The Atomic Force Microscopy (AFM) images of rGO1 and rGO2 are presented in Figures 6a and 6b, respectively. These images clearly demonstrate increased layer separation in rGO2 compared to rGO1. Additionally, the roughness of rGO2 is observed to be higher than that of rGO1. These findings confirm that rGO2 exhibits an improved HTR compared to rGO1, as reported in [7]. This result aligns well with the observations from Raman spectroscopy and UV analysis.

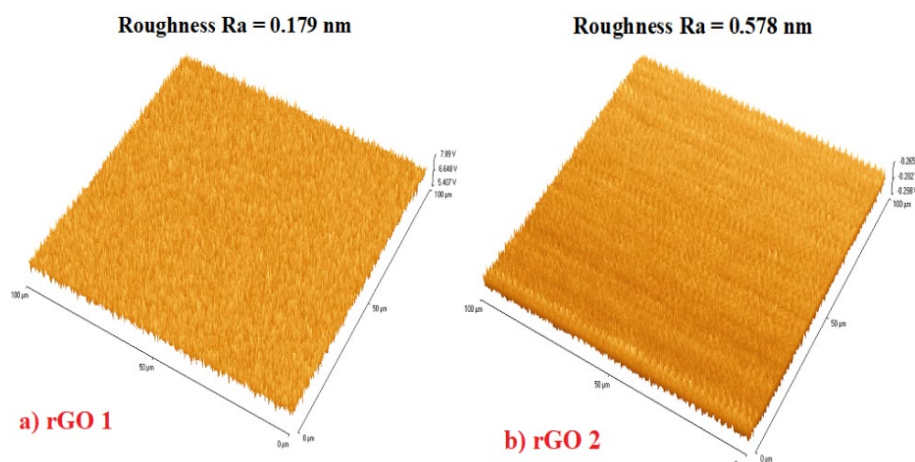


Fig. 6. AFM images for surface furnished rGO 1 and rGO 2 samples.

Fig. 7 demonstrates the UV-Vis absorption spectra of rGO1 and rGO2. For rGO1, absorption peak of GO shifts from 213nm to 259nm, this is explained by the oxygen groups bonded to the graphene layers attached throughout thermal annealing process. In contrast, the rGO2 sample exhibits higher absorption values at 217 nm and 279 nm, indicating that the specific preparation processes resulted in a greater presence of oxygen in the rGO2 sample. While GO nanosheets are hydrophilic, rGO nanosheets are hydrophobic. It was observed that the rGO1 solution remains stable

in deionized water, whereas rGO2 disperses homogeneously in deionized water due to the effects of microwave and ultrasonic treatments [16].

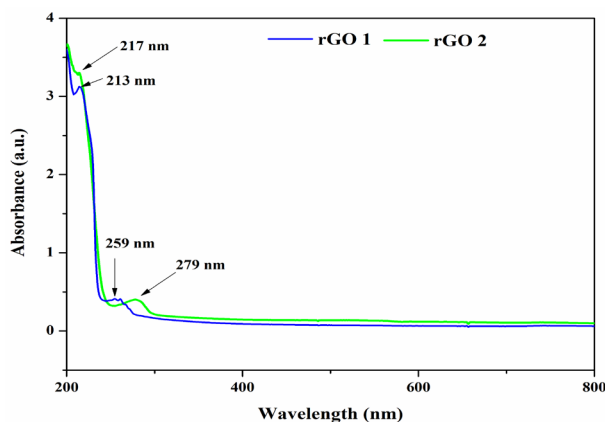


Fig. 7. UV-Vis spectrum of rGO 1 and rGO 2 samples.

3.2. Thermophysical properties and stability of rGO2 nanofluids

In HT applications, thermophysical properties along with stability are important factors. However, the stability of fluids purely relies on their Isoelectric point value (IEPV). Stability of fluid is good when its pH value is distant from IEPV [1,7]. The characterization reports confirm that rGO2 is better than rGO1. The pH meter is utilized to determine pH value of prepared aqua-based rGO2 nanofluids after the 10th day of preparation. Five different trials are carried out for all concentrations (0.0005, 0.001, 0.003, 0.005, 0.007 wt %) and the pH average value is ~ 7.26 , ~ 7.53 , ~ 7.82 , ~ 7.93 , and 8.12 respectively. It is observed that they are distant from the IEPV of rGO2 (~ 4.8), which confirms that the prepared nanofluids have good stability [6]. To conduct the sedimentation study instead of choosing all the prepared concentrations 0.003 wt % is selected as the maximum. The sedimentation study of rGO2 is carried out for 15 days with no sedimentation occurring in the glass tube. An identifiable sedimentation is recorded from the 16th day and extends further; flakes start to establish and the end of the 20th day settle down at bottom of glass tube. Therefore, the prepared rGO2 nanofluids are highly stable for 15 days because of existence of oxygenated groups it is confirmed by FTIR spectroscopy [3-8]. In the prepared rGO2 nanofluids, thermophysical properties and deionized water are exhibited in the Table 1. It is observed that a substantial enhancement in thermal conductivity along with surface tension by the increase in concentration. However, in dynamic viscosity, there is no major change in the concentration of rGO2. Similarly, the density of rGO2 nanofluids decreases in concentrations, and the variation in the concentrations is “insignificant [9].

Table 1. Thermophysical properties of deionized water and rGO aqua nanofluids at 30 °C.

Properties	Deionized water	0.0005 Wt%	0.001 Wt%	0.003 Wt%	0.005 Wt%	0.007 Wt%
Thermal conductivity (W/mK)	0.5984	0.6102	0.6145	0.6162	0.6182	0.6193
Density (kg/m ³)	995.62	994.62	993.32	993.12	992.56	992.42
Surface tension (mN/m)	71.9	72.1	72.3	72.6	72.8	73.2
Dynamic viscosity (mPa s)	0.670	0.674	0.676	0.678	0.679	0.681”

4. Conclusion

In the current study, rGO is modified into rGO1 and rGO2 then its characterization techniques are investigated. In HT applications, stability of the NPs plays a critical role in controlling characteristics of synthesized nanofluids and in specific, stability of the synthesized nanoparticles is comparatively better than that of the purchased one. Hence, this work aims to report a new method of synthesizing rGO nanoparticles for heat transfer applications. Low cost and surfactant free are the significant characteristics of the developed nanofluid. Aqua based rGO2 nanofluids are highly stable for duration of 15days because of existence of oxygenated groups at defective sides. Brownian motion of flakes in base fluid accounts for improvement in the thermal conductivity of synthesized rGO-water nanofluids and all the fluid concentrations represent Newtonian behaviour while no major deviation was noticed in its viscosity. However, surface tension of nanofluid improved with rGO concentrations because of existence of Vander Walls force among accumulated particles at liquid-gas interface. Thus, it can be validated that prepared rGO nanofluids are good in stability and thermophysical properties; also, it is suitable for conventional fluids in the heat transfer applications.

References

- [1] G.J. Lee, C.K. Kim, M.K. Lee, C.K. Rhee, S. Kim, C. Kim., *Thermochim. Acta*, 542, (2012), pp. 24-27; <https://doi.org/10.1016/j.tca.2012.01.010>
- [2] Choi, S. U. S., Eastman, J. A., *ASME Int. Mech. Eng. Congr. Expo.*, (1995), 66, pp.99–105.
- [3] H. Xie, L. Chen, *Phys. Lett., A* 373, (2009), pp. 1861-1864; <https://doi.org/10.1016/j.physleta.2009.03.037>
- [4] P. Estelle, S. Halelfadl, T. Mare, *J. Therm. Eng.* 1, (2015), pp. 381-390; <https://doi.org/10.18186/jte.92293>
- [5] P. Goli, H. Ning, X. Li, C.Y. Lu, K.S. Novoselov, A.A. Balandin, *Nano Lett.* 14, (2014) pp.1497-1503; <https://doi.org/10.1021/nl404719n>
- [6] R. Kamatchi, *J. Heat and Mass Transfer.* (2017); <https://doi.org/10.1007/s00231-017-2135-z>
- [7] R. Kamatchi, S. Venkatachalapathy, B. Abhinaya Srinivas, *International Journal of Thermal Sciences*, 97, (2015), pp. 17-25; <https://doi.org/10.1016/j.ijthermalsci.2015.06.011>
- [8] Divya, P., Barai, Bharat, A., Bhanvasel, Virendra Kumar Saharan., *Ind. Eng. Chem. Res.*,58 (2019), pp. 8349–8369; <https://doi.org/10.1021/acs.iecr.8b05733>
- [9] Haiyan Zhang, Shanxing Wang, Yingxi Lin, Ming Feng, Qibai Wu, *Applied Thermal Engineering.* 119, (2017) pp.132-139; <https://doi.org/10.1016/j.applthermaleng.2017.03.064>
- [10] Leilei Chen, Jian Liu, Xiaoming Fang, Zhengguo Zhang, *Solar Energy Materials & Solar Cells*, 163, (2017) 125-133; <https://doi.org/10.1016/j.solmat.2017.01.024>
- [11] Mahboobeh Hadadian, Elaheh K, Goharshadi, Abbas Youssefi, *J Nanopart Res* (2014) 16:2788; <https://doi.org/10.1007/s11051-014-2788-1>
- [12] S. S. Jyothirmayee Aravind., S., S Ramaprabhu., S, *J. Appl. Phys.* 110 (2011) 124326; <https://doi.org/10.1063/1.3671613>
- [13] Xiaoqiang An, Kimfung Li, Junwang Tang, *Cu2O/Reduced Graphene Oxide Composites for the Photocatalytic Conversion of CO2*; <https://doi.org/10.1002/cssc.201301194>
- [14] Rashmi Chandrabhan Shende, Ramaprabhu., S, *Journal of Nanoscience and Nanotechnology.* 17, (2017), pp. 1233-1239; <https://doi.org/10.1166/jnn.2017.12695>
- [15] Hareema Saleem, Mobeen Haneef, Hina., Y, Abbasi, *Materials Chemistry and Physics* 204 (2018), pp.1-7; <https://doi.org/10.1016/j.matchemphys.2017.10.020>
- [16] Siva Palanisamy, Arunkumar Prabhakaran Shyma, Surendhiran Srinivasan, Naveen Kumar Rajendran, Rajendran Venkatachalam, *Water-dispersible graphene-wrapped MnO2 nanospheres*

and their applications in coin cell supercapacitors, (2019);

<https://doi.org/10.1007/s11581-019-03004-6>

[17] D Vasudevan, D Senthil Kumar, A Murugesan, C Vijayakumar, Experimental investigation and characteristics of multiwalled carbon nanotube aqua nanofluids from a flat plate heater surface in a pool Vol. 68, Iss. 3, (2020): 547-554; <https://doi.org/10.24425/bpasts.2020.133380>

[18] Vasudevan, D., Senthilkumar, D., Surendhiran, S., Int J Thermophys 41, 74 (2020);

<https://doi.org/10.1007/s10765-020-02651-6>